Available online at www.sciencedirect.com
ScienceDirect
Colloids and Surfaces A: Physicochem. Eng. Aspects 304 (2007) 72–76
COLLOIDS AND SURFACES A
www.elsevier.com/locate/colsurfa

Swelling of a single foam film under slipping

J. Emile [a,*], E. Hardy [a,b], A. Saint-Jalmes [a], E. Terriac [a], R. Delannay [a]

[a] Groupe Matière Condensée et Matériaux, UMR au CNRS 6626, Université de Rennes I, Campus de Beaulieu, 35042 Rennes Cedex, France
[b] Laboratoire d'Electronique Quantique-Physique des Lasers, UMR au CNRS 6627, Université de Rennes I, Campus de Beaulieu, 35042 Rennes Cedex, France

Received 14 February 2007; received in revised form 11 April 2007; accepted 15 April 2007
Available online 24 April 2007

Abstract

Aqueous foams are often used under flow, and one of the biggest challenges is to create predictive models of their rheology. Our investigations deal with the problem of slip at surfaces, and more precisely sliding bubbles inside a narrow horizontal tube. Using a new experimental procedure based on a Fabry–Perot interferometer, our first results underline some thickness variations for a vertical film separating two bubbles, and moving horizontally. The velocity-dependent thickness is quantitatively described by a power law. We discuss the possible origins of this effect, and the consistency with available models of bubble slipping. Our observations confirm that, under dynamical conditions, there can be complex liquid re-distribution between the different elements of the foam structure.

Keywords: Aqueous foam; Film thickness; Optical interferometry; Wall slip

1. Introduction

Aqueous foams are complex fluids constituted of tightly packed gas bubbles in a continuous liquid phase. They present original physical and mechanical properties with extensive technological applications including for example oil recovery [1], food formulation [2], detergency [3], as well as new applications emerging like veins treatment in medicine [4] or discrete microfluidics [5,6]. Recent research in foams has focussed on two topics which are often studied separately, but are in fact coupled: stability (liquid drainage, bubble coarsening) and rheology (elastic and viscous behaviors of the foam depending upon the nature of externally applied forces).

Foam rheology [7] can be investigated by many ways: bulk measurements under small amplitude deformation or under steady shear [7,8], Stokes-like experiments [9,10], under extension, etc. Recently, many studies relate to foam-wall friction and slip at surfaces. The occurrence of slip at the fixed boundaries is a major issue in any rheometrical measurement. Different possible geometries can be used to study slipping: directly on macroscopic samples [11,12], or with a train of bubbles inside a tube [13–17]. The latter consists of bubbles, stacked one after the other and flowing inside a narrow tube; it can also be seen as separated thin films pushed inside the tube, connected by a liquid film wetting the tube surfaces. A peripheral Plateau border connects the vertical films separating the bubbles to the tube surface, and to the continuous wetting film at this surface. This set-up has been used to study bubble slipping, and to determine the relationship between their velocity and the viscous friction (or stresses). Experimental and theoretical works have shown for foams, emulsions and bubbles that the bubble-wall friction and the wetting film thickness are represented by power-law functions of the capillary number $Ca = \eta V/\gamma$ where η is the dynamic viscosity of the fluid, V the relative velocity of the bubble to the solid surface and γ the gas–liquid surface tension [12–17]. The relation is not linear (as expected for a simple fluid under shear): as the bubble moves, it notably deforms and the thickness of the wetting film grows. The wetting film and the bubble have thus a complex shape [12,17], which eventually becomes asymmetric. By using the lubrication approximation, the power laws are defined for tangentially perfectly mobile gas/liquid interfaces (zero interfacial viscosity) and tangentially perfectly immobile ones (zero interfacial velocity). In the first case, the viscous dissipation mainly occurs inside the Plateau borders (slow-moving vortex in the Plateau border, and a plug-like flow in the wetting film [17]); and in the second case, the

* Corresponding author. Tel.: +33 2 23 23 56 46; fax: +33 2 23 23 67 17.
E-mail address: janine.emile@univ-rennes1.fr (J. Emile).

0927-7757/$ – see front matter © 2007 Elsevier B.V. All rights reserved.
doi:10.1016/j.colsurfa.2007.04.036

dissipation occurs mostly inside the wetting film. In real situations, interfaces are neither perfectly mobile or immobile; the dissipation can occur in both locations, and the macroscopic behavior is then the result of the balance between the two contributions. One of the assumptions usually made in the models is that the thickness of the vertical bubble film remains constant. Moreover, since the thickness of the bubble films is the order of tens of nm, it is usually neglected when compared to the radius of the Plateau border (few hundred of μm). Despite the fact that the thickness of the wetting film under static conditions has the same order of magnitude than the bubble one, this film cannot be neglected as all the liquid flow is along the wall, and is adequately described by the lubrication approximation. No pressure gradient is considered in the bubble vertical film, which canting angle adjusts to verify the balance of external forces [17]. However, recent works as well as visual observations tend to show that the thickness of the film between bubbles might not be constant in such experiments, or during forced-drainage [18,19], and that there are some dynamical coupling between flow inside Plateau borders, nodes and films [20]. One may then wonder whether it can be accurately measured, and if the thickness variations remain consistent with the assumptions of the existing models.

In this paper, we present new quantitative optical results of the evolution of the thickness of a single vertical bubble film propagating inside a tube. The data show a significant and counter-intuitive swelling with an absolute increase of the thickness by a factor up to two. We thus discuss the impact of this observation on the models, and show that quantitatively, it corresponds to a tiny volume displacement from the Plateau borders, which does not invalidate the models. There is today no theoretical picture for understanding effectively this phenomenon. We just propose here a few ideas on possible mechanisms, mostly linked to the specific geometry of the Plateau border under flow. We then discuss about the impact of this swelling on other issues in foams, as well as about the limit of this first set of experiments.

2. Experimental set-up and procedure

To measure the thickness variations, we use a confocal Fabry–Perot interferometer injected by a monomode Nd:YAG laser operating at $\lambda_0 = 1.064\,\mu m$. The interferometer cavity is made from two identical mirrors of radius of curvature $R_c = 20\,cm$, with intensity reflection coefficient $R = 99\%$ (Fig. 1). The distance between the two mirrors is adjusted such that the cavity is confocal. This interferometer, combined to a Jamin approach [20,21], has been previously used to measure thinning processes of vertical soap films. It allowed to probe simultaneously two points of the film, giving direct access to the thickness gradient. Here, we have restricted our studies using a single beam focussed on the film center.

The liquid solution is prepared from a 20% in volume commercial dish-washing fluid (Apta®) in 65% distilled water. 10% glycerol and 5% cooking sugar are added to strengthen the soap film. The prepared solution is left outside for 1 day in order to evaporate residual alcohol from the mixture. At 23 °C, the dynamic viscosity, is $\eta = 2.1\,mPa\,s$, the surface tension, is $\gamma = 29.9\,mN\,m^{-1}$ and the solution density is $\rho = 1.04 \times 10^3\,kg\,m^{-3}$. From its numerous components and good foaming properties, this solution must have highly viscoelastic interfaces, thus rather low interfacial mobility. Indeed, we have measured that the pressure difference for moving a train of bubbles scales as $Ca^{0.5}$, consistent with immobile surfaces. For the thickness variations studies, a single bubble film is confined in a circular glass tube (length $l = 4\,cm$, diameter $d = 6\,mm$). The film is formed by dipping an end of the tube into the soap solution. Soft rotations are made to evacuate the excess liquid. A syringe pump (PHD 2000, Harvard Apparatus) is connected to the tube (Fig. 1) to push the film by a constant air flow in the range 0.2–3.5 mL min^{-1}. One channel end is at the atmospheric pressure, whereas the other end is enclosed by an optical glass window. Evaporation effects can be neglected as experiments last for less than a minute. Consequently, no control of the vapor pressure was required. The amount of solution

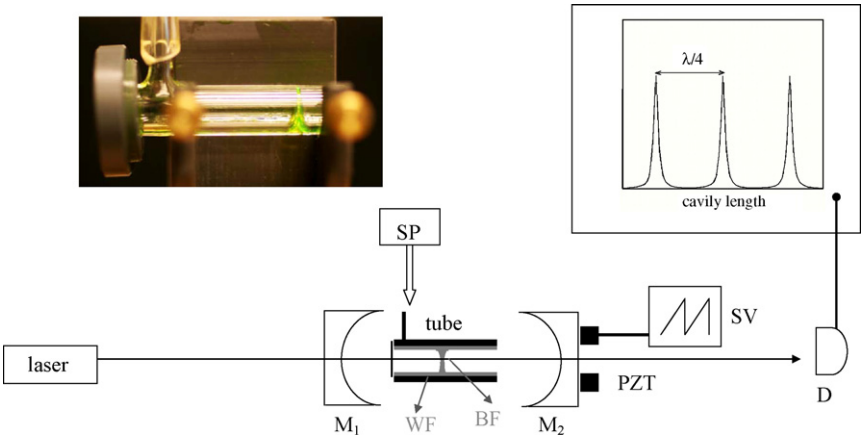

Fig. 1. Experimental set-up. The (Nd:YAG) laser is operated at $\lambda_0 = 1.064\,\mu m$. The Fabry–Perot interferometer is designed with two mirrors (M_1 and M_2). The length of the cavity is scanned by applying a sawtooth voltage (SV) to a piezoelectric transducer (PZT). The output signal is collected by the detector (D). The bubble film (BF) and the wetting film (WF) are schematized by the gray line. The bubble film is pushed with a syringe pump (SP) through a glass tube enclosed by an optical glass window. The insets show the transmitted signal vs. the cavity length and a photography of the bubble film confined in the glass tube, under flow (the film was coloured for the photography).

in the tube is obtained by weighting, and represents only about 1.5% of the tube volume. The motion of the film, which velocity V is constant in the range 0.1–2 mm s^{-1} (corresponding to 7×10^{-6} to 1.4×10^{-4} *Ca* values), is recorded as a function of time using a video camera. The experimental set-up is sealed in a cage to avoid vibration disturbances. The acquisition set-up has a time response of 0.1 s, which is well adapted to the temporal evolution of the film. As the length of the Fabry–Perot cavity is scanned with a piezoelectric transducer, the output signal of the interferometer shows a resonant frequency peak. The thickness evolution of the film is deduced from the free spectral range of the interferometer and is extracted from the peak shift. Data are collected until the film rupture which is considered as the reference state. We check carefully that no frequency shift occurs when an air flux is injected in the empty tube (without film). The finesse F ($F = \Delta\lambda/\delta\lambda$, where $\Delta\lambda$ is the free spectral range and $\delta\lambda$ is the full-width at half-maximum of the peak) of the Fabry–Perot interferometer is 22 for the empty cavity and decreases to 15.5 for the cavity with the soap film. With this method, one can continuously measure the film thickness, whatever its motion or position, as it does not require a focal plane. Some attempts were carried out by trapping two films in the tube but the transmitted signal was always too noisy to hope for quantitative studies of them. The experiments are performed typically in the temperature range of 20–24 °C.

3. Results

3.1. Static case: film drainage

First, we investigate the thickness evolution of a static film confined in the tube. The capillary length $(\gamma/\rho g)^{1/2}$, setting the extension of the peripheral Plateau border, is typically 1.7 mm, so that the height of the flat film is about 3 mm. As the effective diameter of the beam laser is about 1 mm, we are sure that only the middle of the thin film is studied. Note that the system is not vertically symmetric: the Plateau border at the top is thinner than at the bottom. Fig. 2 represents the first steps of the thinning kinetics of the film. The film drains down to about 100 nm (between 110 and 150 nm in average, and much larger than black films) in less than a minute, but required more than 10 min to very slowly reach its final equilibrium thickness of 10 nm. To avoid film rupture and long waiting times which lead to the drying of the wetting film at the tube walls, the film motion experiments are performed rapidly with rather "young" films, only partially drained, at initial thickness of about 100 nm.

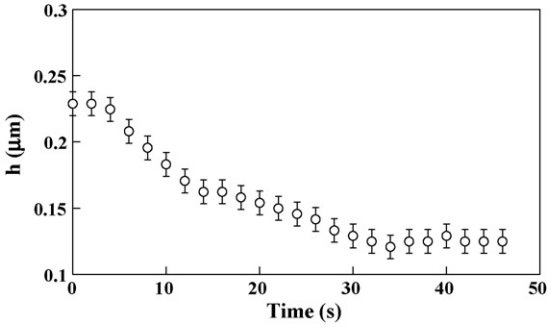

Fig. 2. Effective thickness of the immobile film confined in the tube vs. time. The vertical error bars are linked to the resonant frequency peaks.

The reason for such a slow drainage dynamics is not completely known: in fact, for such bulk and interfacial viscoelastic properties the film should drain faster. It is possible that the presence of the sugar modifies the bulk viscosity inside the film because of the confinement, providing an effective viscosity much higher than the one measured in bulk. Despite significant progress in the understanding of thin liquid films at equilibrium, their drainage kinetics is still not completely understood [23–26]. Variables such as the frame type, size or geometry used to support the suspended film, the nature of surfactant and its concentration, influence the experiments. Moreover, complex effects like dimples and marginal regeneration also occur [23,27,28].

As in previous studies with the same soap solution [22], the thinning process presents a similar complex profile. The first part of the drainage curve actually shows a slow initial rate, and a maximum of the velocity during drainage. This kind of shape has been predicted when considering the viscoelastic nature of the interfaces [29]. In real conditions, as the surface mobility is neither zero nor infinite; surfactants can actually be transported from the interfaces, increasing the mobility during drainage, and thus increasing the drainage speed.

3.2. During film motion

Using the syringe pump, the bubble film is moved at constant velocity in the tube. For air flows below 0.1 mL min^{-1}, the film stays at rest, this is related to some pressure losses in the pipe connecting the syringe to the tube. For higher flow rates, typical data are shown in Fig. 3. When the air is blown, the film presents a curved-like shape and begins to move after a delay time up to 5 s. The origin of this delay time is attributed to the spreading of the wetting film on the glass surface and also to the syringe motor actuation. During this time, i.e. when the film is immobile, the thickness fluctuations remain weak (region 1, Fig. 3). In region 2 where the film moves, we observe a significant shift of the resonant frequency of the transmitted signal. At low veloci-

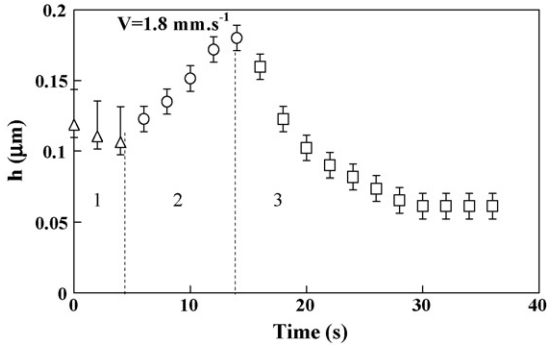

Fig. 3. Temporal evolution of the thickness of the bubble film. The diamond, round and square symbols represent the thickness of the static film (region 1), the film pushed by the air flux and moved at a constant velocity $V = 1.8$ mm s^{-1} (region 2) and the relaxed film (without air blowing, region 3), respectively.

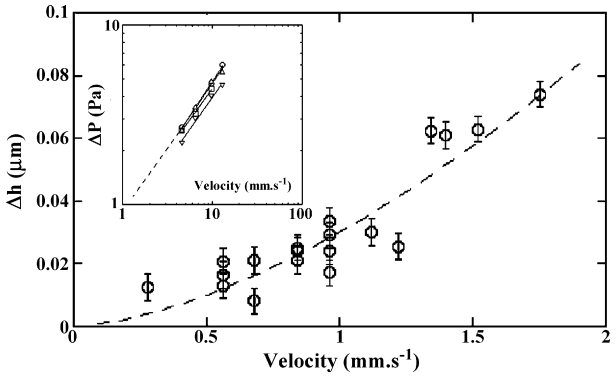

Fig. 4. The thickness evolution of the bubble film Δh as a function of bubble velocity. The data are fitted by an empirical description V^{β} (dotted line), with $\beta \approx 1.5$. The insert shows the pressure drop ΔP of the bubble film vs. velocity using the experimental set-up of Ref. [16]. The curves refer to various liquid fractions.

ties, the thickness reaches a maximum value h_{max} with a steady state (lasting up to 30 s for the smallest speed $V = 0.5\ \mathrm{mm\ s^{-1}}$), before stopping the syringe pump. The effective length of the tube ($l_{eff} = 3$ cm) imposed by the optical equipment in order to stay in the Rayleigh range and the outflow position (1 cm from the open-end, Fig. 1) limits the range of the studied velocities and of the time of measurements. Several measurements were carried out to be ensured of the reproducibility of the data. The steady state corresponding to the value of 0.18 μm persists during approximately 4 s, even when the syringe pump is stopped. When the air blowing is stopped (region 3), the film stops and its thickness relaxes to a constant value always inferior to the initial one. The moving film loses liquid during its passage to wet the walls of the tube and the final thickness observed in the region 3 depends on displacement.

For the studied velocity range, the absolute variations of the film thickness $\Delta h = h_{max} - h_i$, where h_i is the initial thickness, are reported in the Fig. 4. The data are fitted by an empirical description $\Delta h = \alpha V^{\beta}$ giving parameters $\alpha \approx 3 \times 10^{-4}$ and $\beta \approx 1.5$. After stopping the motion, the lifetime of the film is strongly shortened with a spontaneous rupture. Many measurements have been made to verify the reproducibility.

Lastly, using the same experimental set-up of the reference [16], the pressure drop ΔP of a single bubble film in a millimetric channel (length = 30 cm, diameter = 4 mm) has been measured with a pressure sensor as a function of the velocity. Different from the case of a train of bubbles [16], the pressure drop does not scale with $Ca^{1/2}$, but an exponent 0.73 ± 0.03 (insert of Fig. 4) is found. This result will be studied and discussed in details in [30], and rises questions about the existing analogy between a system of a single film, and a system consisting of many films (bubble train).

4. Discussion

The observation of the swelling of the vertical film is rather unexpected. Indeed, if one considers that the film motion implies an increase of the wetting film thickness, to the expense of the Plateau border, one may then expect a thinning of the vertical bubble film. As the Plateau border shrinks, its radius of curvature decreases and thus the capillary suction on the film is higher. But one observes the opposite fact: the Plateau border provides liquid to the wetting film, but can also distribute liquid to the vertical bubble one.

The swelling of the vertical film may be explained by the distortion of the Plateau border profile. It is predicted and observed [12,17] that its shape is strongly modified by the drag of liquid into the wetting film, and even becomes asymmetric with different curvature radii on both sides of the film. The details of this asymmetry induced by the flow must be taken into account, and the problem cannot be treated by a single mean effective value.

The shape of the Plateau border is assumed to be deformed with different radius of curvature, $(r - \varepsilon)$ at the front and $(r + \varepsilon)$ at the back sides ($\varepsilon \ll r$). Considering only the static Laplace pressure differences, one gets a pressure drop $\Delta P \sim -2\varepsilon\gamma/r^2$ between the two sides of the film This static approach thus implies a negative ΔP, which does not match with the actual film curvature. In order to have a $\Delta P > 0$, one must then introduce a dynamic pressure P_d in the fluid: $\Delta P \sim -2\varepsilon\gamma/r^2 + P_d$. The origin of this dynamic pressure P_d results from the flow induced by non-uniform surfactant concentrations at the Plateau border interfaces. Indeed, at the front, the surfactant are more stacked and compressed, while they are more expanded at the back. Such surface tension gradients create Marangoni flows with surfactant transfer across the border and the film to stabilize the depleted surfactant area. Eventually, this complex diffusion-driven hydrodynamic flow implies an upward motion and an increase of the film thickness. As the viscous force per unit length of Plateau border is proportional to Ca^{α}, (here we have found $\alpha = 0.73$) we can write that $\varepsilon \sim -Ca^{\alpha} + r^2 P_d/2\gamma$. We assume that the volume of liquid which goes to the film is simply proportional to the one lost by the Plateau border: $\Delta h d^2 \sim \varepsilon^2 d$, with the tube diameter d. From these different relationships, one gets $\Delta h \sim V^{2\alpha}$, with considering that P_d does not depend on V. After all these crude assumptions, one gets an exponent $2\alpha \sim 1.46$, close to the one found in Fig. 4. But we still do not know the details of the creation of the dynamical pressure P_d. In that respect, such experiment could be used to understand better the occurrence of dynamical pressure in confined flows, and its dependence with the flow parameters.

For the studied velocity range ($V \approx 1\ \mathrm{mm\ s^{-1}}$), the maximum swelling of the bubble film $\Delta h \approx 100$ nm leads to a excess of liquid which actually results from a tiny constriction of the Plateau border. Indeed, the amount of liquid in the Plateau border can be estimated by its volume $V_{PB} \approx \pi(2 - \pi/2)r^2 d$, with the curvature radius of the Plateau border r. As the radius of the Plateau border is at least 300 μm (width of the upper meniscus, $2r$, measured by optical microscope), the constriction corresponds to a liquid loss from the Plateau border of 0.4% of its initial volume. Note that relatively, the swelling of the bubble film is even smaller if one considers wetter foams (larger Plateau border radius), while keeping the same liquid loss. In terms of volume transported, this effect is thus quite small. Moreover, when compared to the swelling of the wetting film (which thickness varies of a few microns), this vertical film swelling can actually be neglected. This validates the main assumptions made in models [12–14,17].

It is also important to note that the experimental time of these experiments (less than 1 min) is much smaller that the drainage time (more than 10 min). For longer times of measurement, the drainage could modify the final evolution thickness. As mentioned previously, the steady state was observed during at least 30 s for the lowest velocities, without tracing any effect of the drainage. But, as we were limited by the configuration of the device, it is difficult to exclude the existence of this contribution and to state that we have measured the final equilibrium state. Concerning the smaller thickness obtained after stopping the film, it is due to the fact that the moving film loses liquid during its passage to wet the walls of the tube.

In that respect, there are still many open issues and possible other new measurements. One can then wonder about the role of the surfactants (acting both on the interfacial mobility and drainage time), on the role of the initial thickness, or on the number of films (is this effect also seen for every film stacked in a train, or it is simply linked to the first one?). The possible importance of the film section variation during motion, as well as the impact of the vertical asymmetry must also be investigated.

Nevertheless, at this stage, these results clearly evidence the idea that under dynamical conditions, there are some liquid redistribution from the Plateau borders (main reservoirs) to its attendant nodes and films. Such liquid transfer and variable film thickness may play an important role in many other issues: for instance, concerning the dissipation mechanisms controlling the $G''(\omega)$ (loss complex shear modulus) of a foam [31], the local neighbour-switching topological changes (T1 events) [32] or the velocity profiles in confined geometries [33,34]. Furthermore this effect may influence the foam stability under shear, for which the probability of film rupture must decrease and other foam behaviors, including convective instabilities [35,36] or dilatancy effects [37,38].

5. Conclusion

In summary, we have presented an experimental and accurate set-up for measuring vertical bubble film drainage, and film swelling during its motion in a narrow channel. In situ measurements show that the bubble film thickens when it starts to slip on a wetting film. The subject remains open, namely how the films in a foam in permanent flow evolve. At any sliding motions of the bubbles along a smooth wall, the approximation of keeping the film at constant small thickness remains valid: the increase of film volume always corresponds to less than 1% of the Plateau border volume. The swelling is distinctly described by a power law function which must be defined for high *Ca* values.

The interplay between the geometry of the different foam structures (Plateau border, nodes and films), the balance of viscous dissipation in these structures, and the macroscopic behavior still deserves some attention. Further work on the flow in isolated structures are needed, and should help to increase our understanding of the flow of aqueous foams.

Acknowledgments

The measurements of the liquid film thickness evolutions have been done at the Laboratoire d'Electronique Quantique-Physique des Lasers, UMR au CNRS 6627, Université de Rennes I, using the interferometer developed by this team. The authors would like to thank G. Ropars, I. Cantat, D. Chauvat, and A. Le Floch for their help and constructive discussions.

References

[1] M. Chen, Y.C. Yortsos, W.R. Rossen, Phys. Rev. E 73 (2006) 036304.
[2] J. Kokini, G.A. Van Aken, Food Hydrocoll. 20 (2006) 438.
[3] R.S. Powale, A.P. Andheria, S.S. Maghrabi, S.S. Bhagwat, J. Dispersion Sci. Technol. 26 (2005) 597.
[4] N.S. Sadick, Dermatol. Clin. 23 (2005) 443.
[5] W. Drenckhan, S.J. Cox, G. Delaney, H. Holste, D. Weaire, N. Kern, Colloids Surf. A 263 (2005) 52.
[6] J.P. Raven, P. Marmottant, F. Graner, Eur. Phys. J. B 51 (2006) 52.
[7] R. Höhler, S. Cohen-Addad, J. Phys.: Condens. Matter 17 (2005) R1041.
[8] A. Saint-Jalmes, D.J. Durian, J. Rheol. 43 (1999) 1411.
[9] I. Cantat, O. Pitois, Phys. Fluid 18 (2006) 083302.
[10] B. Dollet, F. Elias, C. Quilliet, C. Raufaste, M. Aubouy, F. Graner, Phys. Rev. E 71 (2005) 031403.
[11] L. Bécu, P. Grondin, A. Colin, S. Manneville, Colloids Surf. A 263 (2005) 146.
[12] N.D. Denkov, S. Tcholakova, K. Golemanov, V. Subramanian, A. Lips, Colloids Surf. A 282 (2006) 329.
[13] F.P. Bretherton, J. Fluid Mech. 10 (1961) 161.
[14] L.W. Schwartz, H.M. Princen, A.D. Kiss, J. Fluid Mech. 172 (1986) 259.
[15] I. Cantat, N. Kern, R. Delannay, Europhys. Lett. 65 (2004) 726.
[16] E. Terriac, J. Etrillard, I. Cantat, Europhys. Lett. 74 (2006) 209.
[17] A. Saugey, W. Drenckhan, D. Weaire, Phys. Fluids 18 (2006) 053101.
[18] V. Carrier, S. Destouesse, A. Colin, Phys. Rev. E 65 (2002) 061404.
[19] O. Pitois, C. Fritz, M. Vignes-Adler, J. Colloid Interface Sci. 282 (2005) 458.
[20] A. Saint-Jalmes, Soft Matter 2 (2006) 836.
[21] D. Chauvat, C. Bonnet, A. Durand, M. Vallet, A. Le Floch, Opt. Lett. 28 (2003) 126.
[22] G. Ropars, D. Chauvat, A. Le Floch, M.N. O'Sullivan-Hale, R.W. Boyd, Appl. Phys. Lett. 88 (2006) 234104.
[23] K.J. Mysels, K. Shinoda, S. Frankel, Soap Films. Studies of their Thinning and a Bibliography, Permagon Press, New York, 1959.
[24] V. Bergeron, J. Phys.: Condens. Matter 11 (1999) R215.
[25] S. Stoyanov, N. Denkov, Langmuir 17 (2001) 1150.
[26] S. Berg, E.A. Adelizzi, S. Troian, Langmuir 21 (2005) 3867.
[27] A. Aradian, E. Raphaël, P.G. De Gennes, Europhys. Lett. 55 (2001) 834.
[28] G. Singh, C.A. Miller, G.J. Hirasaki, J. Colloid Interface Sci. 187 (1997) 334.
[29] D. Tambe, M.M. Sharma, J. Colloid Interface Sci. 147 (1991) 137.
[30] E. Terriac, J. Emile, A. Saint-Jalmes, publication in progress.
[31] D.M.A. Buzza, C.Y.D. Lu, M.E. Cates, J. Phys. II France 5 (1995) 37.
[32] J. Lauridsen, G. Chanan, M. Dennin, Phys. Rev. Lett. 93 (2004) 018303.
[33] Y. Wang, K. Krishan, M. Dennin, Phys. Rev. E 73 (2006) 031401.
[34] E. Janiaud, D. Weaire, S. Hutzler, Phys. Rev. Lett. 97 (2006) 038302.
[35] S. Hutzler, D. Weaire, R. Crawford, Europhys. Lett. 41 (1998) 461.
[36] M.U. Vera, A. Saint-Jalmes, D.J. Durian, Phys. Rev. Lett. 84 (2000) 3001.
[37] S.P.L. Marze, A. Saint-Jalmes, D. Langevin, Colloids Surf. A 263 (2005) 121.
[38] D. Weaire, S. Hutzler, Phil. Mag. 83 (2003) 2747.